

Cite this: DOI: 10.1039/c0xx00000x

www.rsc.org/xxxxxx

ARTICLE

# Transition metal ion-substituted polyoxometalates entrapped into polypyrrole as electrochemical sensor for hydrogen peroxide

Nargis Anwar,<sup>a</sup> Mikhail Vagin,<sup>a</sup> Fathima Laffir,<sup>b</sup> Gordon Armstrong,<sup>b</sup> Calum Dickinson<sup>b</sup> and Timothy McCormac<sup>\*a</sup><sup>5</sup> Received (in XXX, XXX) Xth XXXXXXXXX 20XX, Accepted Xth XXXXXXXXX 20XX

DOI: 10.1039/b000000x

A conducting polymer was used for the immobilization of various transition metal ion-substituted Dawson-type polyoxometalates (POMs) onto glassy carbon electrodes. Voltammetric responses of films of different thicknesses were stable within the pH domain 2-7 and reveal redox processes associated with the conducting polymer, the entrapped POMs and incorporated metal ions. The resulting POM doped polypyrrole films were found to be extremely stable towards redox switching between the various redox states associated with the incorporated POM. An amperometric sensor for hydrogen peroxide detection based upon the POM doped polymer films was investigated. The detection limits were 0.3 and 0.6  $\mu\text{M}$ , for the  $\text{Cu}^{2+}$ - and  $\text{Fe}^{3+}$ -substituted POM-doped polypyrrole films respectively, with a linear region from 0.1 up to 2mM  $\text{H}_2\text{O}_2$ . Surface characterization of the polymer films was carried out using atomic force microscopy, x-ray photoelectron spectroscopy and scanning electron microscopy.

## Introduction

Polyoxometalates (POMs) are a widely increasing class of inorganic early transition metal-oxide clusters. The structural and compositional diversity among this class of compounds have enabled them to be promising candidates for a wide range of applications across material science, medicine, biotechnology, nanotechnology and catalysis.<sup>1-12</sup> The general structure of POMs consists of  $\text{MO}_6$  units joined together by edge or corner sharing and connected tetrahedrally to a centrally bonded heteroatom (usually phosphorus or silicon). One of the  $\text{MO}_6$  units can be removed from the structure at higher pH and substituted with different metal ions allowing for controllable molecular design.

Various strategies have been used for immobilization of POMs onto different surfaces, safeguarding their inherent properties. These include: sol-gel technique,<sup>13</sup> adsorption,<sup>14</sup> electrodeposition,<sup>16, 17</sup> monolayers,<sup>18</sup> layer-by-layer self assembly<sup>19</sup> and entrapment into conducting polymers.<sup>20, 21</sup> Among several properties of polyoxometalates, the most interesting one is their ability to accept multiple electrons reversibly during their various redox processes.<sup>10</sup> This ability allows them to behave as excellent electrocatalysts. Consequently, immobilization of these compounds onto different electrode surfaces is very important to explore their electrocatalytic abilities towards analytes of interest.

The most suitable approach for electrode surface confinement of POMs is an incorporation of them into a conducting polymer matrix, which can be done by two methods. The first approach involves the covalent modification of already synthesized polymer film at the electrode surface with the POM.<sup>22</sup> The second method is based on the usage of POMs as dopants during the electropolymerization. Sung et al. incorporated  $[\text{SiW}_{12}\text{O}_{40}]^{4-}$  and

$[\text{P}_2\text{W}_{18}\text{O}_{62}]^{6-}$  into polypyrrole and did not observe any leaching effect during redox switching with charge compensation during polymer reduction being comprised of cation injection from solution.<sup>21</sup> Poly(3-methylthiophene) was used as a polymer matrix for the incorporation of Keggin-type POMs such as  $\text{PW}_{12}\text{O}_{40}^{3-}$ ,  $\text{SiW}_{12}\text{O}_{40}^{4-}$ ,  $\text{PMo}_{12}\text{O}_{40}^{-}$  by G. Bidan *et al.*<sup>20</sup> Liu and Dong entrapped a molibdosilic heteropoly complex with dysprosium into a polypyrrole matrix.<sup>23</sup> McCormac *et al.* have immobilized a series of Dawson-type POMs into polyvinylpyridine, polypyrrole and poly(N-methylpyrrole).<sup>24</sup> They obtained stable parent Dawson POM-doped polypyrrole films by restricting the cycled potential limits to the first two tungsten-oxo based redox processes. They also reported stable  $\text{Cu}^{\text{II}}$ -substituted POM-doped polypyrrole films for the first time and showed that poly(N-methylpyrrole) is the most suitable conducting polymer for the immobilization of  $\text{Fe}^{3+}$ -substituted POM. Dong *et al.* also incorporated Dawson-type POMs into a polypyrrole matrix.<sup>25</sup> Remarkable enhancement of electrocatalytic oxygen reduction was obtained with certain POM-doped polypyrrole films.

Reliable, simple and low-cost systems for hydrogen peroxide detection are attractive for biomedical and environmental applications as well as for industrial control. Alternatively, blood glucose monitoring devices often include the hydrogen peroxide sensors as transducers for glucose measurements.<sup>26</sup> Methods of hydrogen peroxide detection include chemiluminescence,<sup>27, 28</sup> fibre optics devices,<sup>29</sup> fluorimetry,<sup>30</sup> and electrochemical tools.<sup>31-33</sup> Different examples of electrode modifiers that possess the advantages of electrochemical detection for hydrogen peroxide, such as low-cost, reliability and simplicity, include Prussian blue,<sup>34, 35</sup>  $\text{Fe}_3\text{O}_4$ ,<sup>36</sup> vanadium-doped zirconias<sup>37</sup> and

polyoxometalates.<sup>38, 39</sup> Despite the high selectivity and sensitivity of enzyme-modified electrodes,<sup>40, 41</sup> the limitation of usage of these systems is related to the difficulty in obtaining the optimal conditions and the lack of the enzymatic activity over a period of time,<sup>42</sup> which makes them less attractive. Owing to their inherent characteristics, POMs are presented as excellent candidates for electrocatalytic reduction of hydrogen peroxide.<sup>43-45</sup> In order to prepare chemically modified electrodes for electrocatalytic reduction of H<sub>2</sub>O<sub>2</sub>, POMs have been immobilized onto modified silica gel,<sup>46</sup> multilayer assemblies<sup>47, 48</sup> or ordered mesoporous carbon.<sup>49</sup>

In this work, transition metal-substituted Dawson-type POMs were immobilized via doping ion insertion during the electropolymerization of polypyrrole. Redox processes associated with the W-O redox sites and the transition metal centres of the POMs inside the polymer matrix were accessible for voltammetric studies in acidic medium. The films exhibited stable redox responses in the pH range of 2-7. Surface characterization was carried out using the AFM, XPS and SEM. Electrocatalytic activity of the films containing iron and copper-substituted POMs towards the reduction of hydrogen peroxide was studied by amperometry at physiological conditions (pH 6.5) and compared with the performance of the same POMs in solution<sup>50</sup> and immobilized onto an electrode surface via multilayer assemblies.<sup>19</sup> Conducting polymer-based POM-doped polypyrrole films reveal the best analytical characteristics for hydrogen peroxide reduction in comparison with some other approaches.

## Experimental

### Materials

The potassium salts of all the substituted Dawson type polyoxometalates investigated were synthesized and characterised by both electrochemical and spectroscopic techniques as described previously.<sup>51</sup> All other chemicals were of reagent grade, purchased from Aldrich and were used as received unless otherwise stated. Sulphuric acid (95-97%) was received from Riedel-de-Haen. Pyrrole (99%) was received from ACROS Organics and purified before use by passing through a neutral Al<sub>2</sub>O<sub>3</sub> column to obtain a colourless liquid. Alumina powders of sizes 0.05, 0.3 and 1.0 μm were received from CHI Instruments. Water was purified using Milli-Q water purification system. Stock solutions of H<sub>2</sub>O<sub>2</sub> (0.25M) were freshly prepared before use from a 30% solution. Buffer solutions were prepared from the following solutions, which were either adjusted with 0.1M NaOH or 0.1M H<sub>2</sub>SO<sub>4</sub>, 0.1M Na<sub>2</sub>SO<sub>4</sub> (pH 2 to 3), 0.1M Na<sub>2</sub>SO<sub>4</sub>, 0.02M CH<sub>3</sub>COOH (pH 3.5 to 5) and 0.1M Na<sub>2</sub>SO<sub>4</sub>, 0.02M NaH<sub>2</sub>PO<sub>4</sub> (pH 5.5 to 7).

### Apparatus and Procedures

All electrochemical experiments were performed with the CHI660 electrochemical work station in a conventional three-electrode electrochemical cell using a glassy carbon electrode (GCE, 3mm diameter and Area 0.0707 cm<sup>2</sup>) as the working electrode, a platinum wire as the auxiliary electrode, and an Ag/AgCl as the reference electrode in aqueous media. The GCE

was polished with 1.0, 0.3 and 0.05 μm Al<sub>2</sub>O<sub>3</sub> powders, successively, and sonicated in water for about 10 min after each polishing step. Finally, the electrode was sonicated and washed with ethanol, then dried with a high purity argon stream immediately before use. Solutions were degassed for at least 20 min with high-purity argon and kept under a blanket of argon during all electrochemical experiments.

POM-doped polymer films deposited on ITO slides were characterised using X-ray photoelectron spectroscopy (XPS). Analysis was performed in a Kratos AXIS 165 spectrometer using monochromatic Al Kα radiation of energy 1486.6 eV. High resolution spectra were taken at fixed pass energy of 20 eV. In the near-surface region the atomic concentrations of the chemical elements were evaluated after subtraction of a Shirley type background by considering the corresponding Scofield atomic sensitivity factors. Surface charge was efficiently neutralised by flooding the sample surface with low energy electrons. Core level binding energies were determined using C 1s peak at 284.8 eV as the charge reference.

Atomic force microscopy was conducted in AC ('tapping') mode on an Agilent 5500 controlleld using PicoView 1.10.1 software. Micromasch NSC15 or Olympus AC 160 TS cantilevers having tetrahedral tips of radius < 10 nm with a resonant frequency of 325 kHz or 300 kHz, respectively, were used.

The areas of interest examined and image sizes used for each sample were chosen based on the expected dimensions of the features of interest identified from SEM analysis. Multiple areas were imaged on each sample to ensure that the high resolution images presented here were representative of the entire sample. Scan speeds were optimized to suit the features observed for each sample.

All images presented were obtained at 512 pixel resolution. Image analysis was undertaken using PicoImage Advanced 5.1.1 software. The raw topography and amplitude data was leveled, noise was removed by applying a spatial filter, and line noise arising from artefacts were removed where necessary. Height Parameters for each sample were determined according to ISO 25178. The resulting topography and amplitude profiles are presented as pseudo-colour images below.

Scanning Electron Microscopy (SEM) of the polymer films was performed on a Hitachi SU-70 FESEM using accelerating voltages of 3 kV and 20 kV. Films were deposited onto ITO coated glass slides for recording the SEM images. Films were uncoated as a low voltage (3kV) was employed to avoid charging effects during imaging. Energy Dispersive Spectroscopy (EDS) used an Oxford Instruments SDD X-max detector with 50 mm<sup>2</sup> window and operated at accelerating voltage of 20 kV.

### Polymer Immobilization

A previously reported procedure was employed after modifications for the electrochemical surface immobilization of polypyrrole on the GCE using potassium salts of transition metal (Fe<sup>3+</sup>, Cu<sup>2+</sup>, Co<sup>2+</sup>) substituted Dawson polyoxometalates as the polymer's dopant anion.<sup>24</sup> The films were grown at a constant potential of +0.65V in a solution containing 0.1M pyrrole and 5mM POM. The deposition process has been controlled by chronocoulometry of different charges (10, 20 and 30 mC). Prior

to further studies, the polymer modified electrodes were washed with a buffer solution prior to use.

## Results and Discussions

### Solution electrochemistry of POMs

In base solution, Dawson-type POMs lose one tungsten-oxo group and leave a lacuna in the cage structure. Transition metal ions can enter the defect and combine with five bridging oxide anions. Figure 1 represents the cyclic voltammograms of different POMs at different stages of transition metal ion insertion. It can be observed at Figure 1A that cyclic voltammogram of the parent Dawson possesses both single and multiple electron redox waves which correspond to the redox activity of the tungsten-oxo centers within the heteropolyanion. The Dawson structure can possess a charge of -8 without protonation in acidic solutions and that the reduction of the Dawson anion involves the addition of up to six electrons.<sup>5</sup> Redox peak couples I and II represent two single-electron pH-independent processes, whereas couples III and IV represent bielelectronic pH-dependent redox transfers. The lacunary Dawson-type anion (Fig. 1B) reveals the set of three, bielelectronic redox processes.<sup>5</sup> The anodic peak of redox process I splits into two peak couples depending on the voltammetry limits. This likely corresponds to the presence of some impurities or the instability of the anion. Peaks of couples II and III are less-defined and more-separated with respect to the parent Dawson. All these observations show instability of the lacunary Dawson-type anion in solution. The insertion of an Fe<sup>3+</sup> ion into the defect of the lacunary POM shows the appearance of a well-defined redox peak couple corresponding to the Fe<sup>II/III</sup> single-electron redox process with an E<sub>1/2</sub> of +0.045 V (vs Ag/AgCl).<sup>5</sup>

### Surface Immobilization of POMs

The conducting polymer polypyrrole was chosen as the supporting conductive matrix for the surface immobilization of the transition metal ions-substituted Dawson-type POMs. Figures 2(A, B and C) represent the resulting electrochemical behaviour of polypyrrole films doped with the Fe<sup>3+</sup>-, Cu<sup>2+</sup>- and Co<sup>2+</sup>-substituted Dawson POMs respectively. All cyclic voltammograms show three typical bielelectronic redox couples W1, W2 and W3 corresponding to the W-O centers within the POM. It is seen from the increase of capacitive currents between two nearby peaks, that only the W1 redox process appears in the conducting region of the polypyrrole backbone, whilst the processes W2 and W3 are in the polymer's insulating region. The metal redox sites appear in the conducting region of the polymer. The anodic and cathodic peak currents of the stable W2 couple are linear with scan rates up to 75mV/s, this being indicative of a surface-confined species. The electrode processes became controlled by proton diffusion into the polymer film at higher scan rates. The peaks are well-defined and less-separated with respect to the lacunary Dawson and Fe<sup>3+</sup>-substituted Dawson in solution. Continuous cycling of the polymer-modified electrode through the various redox processes results in a small decrease in the associated currents. This being indicating the inherent stability of the POM anions within the polypyrrole matrix.

Figure 2A shows the redox couple (E<sub>1/2</sub> of 0.07 V (vs Ag/AgCl)) associated with the POM's Fe<sup>II/III</sup> redox centre. In Figure 2B, only the anodic peak of the Cu<sup>0</sup> to Cu<sup>2+</sup> process is

seen (E<sub>p</sub> of 0.15 V (vs Ag/AgCl)) while the reduction of the Cu<sup>2+</sup> is seen to overlap with the first W-O based reduction peak, which results in a higher reduction peak current for the W1 process of the Cu<sup>2+</sup>-POM-doped film, with respect to the Co<sup>2+</sup>-POM-doped film.<sup>5</sup> This behaviour is also observed in solution for the Cu<sup>2+</sup>-substituted POM. The Co<sup>2+</sup> redox centre is not seen in Figure 2C, as it is present in the region where the polymer is overoxidized and is not accessible.<sup>5</sup>

The E<sub>1/2</sub> values of all these metal centres, and associated redox W-O sites, are in close agreement with solution behaviour of these POMs. The values of ΔE<sub>p</sub> obtained for the redox metal centres and the W-O frameworks at film-modified electrodes are typical for surface confined species. The values of the full width half maxima of the peaks corresponding to metal centres and W-O frameworks deviate from the deal value of 45.3 mV for the W-O bielelectronic redox processes and 90.6 mV for the monoelectronic metal based redox processes. This has been observed previously for other POM-based surface films<sup>42</sup> and is due to repulsive interactions between the surface confined redox sites.

The quantities of the immobilized POMs in the polymer films was calculated by W2 peak current integration at a slow scan rate. The various POM-doped film-modified electrodes exhibited similar coverages of 2.8 nmol cm<sup>-2</sup> for Fe<sup>3+</sup>-substituted, 2.7 nmol cm<sup>-2</sup> for the Cu<sup>2+</sup>-substituted and 1.4 nmol cm<sup>-2</sup> for the Co<sup>2+</sup>-substituted Dawson-doped polymer film.

### Effect of Solution pH

It is well known that POMs exhibit pH dependant electrochemical redox processes both in the solution and surface states.<sup>52-54</sup> McCormac *et al.* have previously shown that the metal ion-substituted Dawson POMs possess pH dependant single and multiple electron redox processes.<sup>5</sup> Figure 3 shows the pH dependencies of voltammetric response of electrodes modified with polypyrrole doped with the Fe<sup>3+</sup>-substituted POM. The number of protons associated with each redox process can be obtained from the slope of the pH dependencies of the formal potentials. The values of slopes for the W2 (70 mV/pH unit) and W3 (63 mV/pH unit) redox couples clearly show that 2 protons are involved in these processes. However the slope for the W1 couple (31 mV/pH unit), which is located in the polymer's conducting region, is smaller than expected possibly due to the repulsive interactions between the polymer backbone and the incoming protons.<sup>55</sup>

### Surface analysis of POM doped polypyrrole films

#### XPS studies of POM doped polymer films

Surface composition of the deposited films was determined by performing X-ray photoelectron spectroscopy (XPS) on POM-doped polypyrrole coated ITO glass slides. The high resolution C 1s and N 1s spectra confirm the presence of polypyrrole. The C 1s spectra can be decomposed into two major peaks to represent C-C/C=C at 284.8 eV and C-N of the polypyrrolic chains at 286 eV, and two minor peaks at 287.5 and 289 eV to represent oxidised carbon. The N 1s spectra can be decomposed mainly into 2 component peaks. The lower binding energy peak at 399.9 eV is attributed to neutral nitrogen in polypyrrole and the peak at

binding energy greater than 401 eV is attributed to protonated nitrogen. The ratio of N<sup>+</sup>/N(total) for Fe<sup>3+</sup>-, Cu<sup>2+</sup>- and Co<sup>2+</sup>-doped polymer are 0.22, 0.41 and 0.66 respectively and could give an estimate of the doping levels. The presence of the dopant is evident from the presence of W, O and P and in the case of Cu-POM doped polypyrrole films, presence of Cu. As far as metals are concerned only Cu is observed, but no Fe or Co were detected. The metal species are in most cases present in very low atomic concentrations considering that they are present as part of a huge complex made of many atoms. In samples, where the metal species could not be identified, it may be that they are present in concentrations below the detection limit of the instrument (~ < 0.1 atomic %).

#### AFM imaging of the polymer films

AFM imaging of POM-doped polypyrrole coated ITO glass slides was performed to find out the topography of the films. Figure 4A presents the AFM image of the Co<sup>2+</sup>-POM-doped polymer film. Root mean square surface roughness parameters were 29.4 nm, 16.8 nm and 13.5 nm for Fe<sup>3+</sup>-, Cu<sup>2+</sup>- and Co<sup>2+</sup>-doped polymer films respectively, which are in agreement with data reported previously.<sup>56-58</sup> Consistent with the SEM results, globular features were observed within the AFM topography images of all polymer films with different sizes. The diameter of these globules varied significantly both within the same film and between the films. Similarly, significant variation was seen in the apparent film thickness. These structures had an overall hemispherical shape, which may be most readily seen in the amplitude (height) images. Little phase contrast was seen for all the films analysed; this suggests that the samples consisted of a homogenous polymer film within the areas of interest imaged.

#### SEM imaging of the POM doped polymer films

Figure 4B shows the SEM image of a Co<sup>2+</sup>-doped polypyrrole film with a charge deposition 10mC. Due to deposition charge the film was not very thick and appeared like a thin layer on the ITO coated glass slide. The SEM image reveals large 400-500 nm particles that were seen as part of a film with low separation between particles. Small particles, < 50 nm, could also be seen decorating the surface of the larger particles. Fe<sup>3+</sup>-, Cu<sup>2+</sup>-POM doped polypyrrole films reveal the same surface morphology. Some micron sized circular islands of the films can still be seen formed by similar sized particles. EDX results of the same films also confirmed the elements present and showed the presence of W, C, N and O, which is in good agreement with the XPS results. No metals in the POMs were again not seen, and is possibly due to the high accelerating voltage used on the thin film and the relatively low concentration of the metals. The presence of tungsten, which is more concentrated than the Fe, Co and Cu, does indicate that the POM is present.

#### Catalytic properties of the POM doped polypyrrole films

##### Cyclic Voltammetry

Polyoxometalates have previously been employed for the reduction of hydrogen peroxide<sup>43-45</sup>. Here both the Fe<sup>3+</sup>- and Cu<sup>2+</sup>-substituted Dawson-doped polypyrrole films were studied

for the electrocatalytic reduction of hydrogen peroxide. All investigations were conducted in pH 6.5 in order to use the sensors in physiological conditions. Figure 5 shows the cyclic voltammograms of stable redox process obtained for the Fe<sup>3+</sup>-POM-doped polypyrrole film-modified electrode in the absence and presence of successive amounts of H<sub>2</sub>O<sub>2</sub>. The reduction peak currents increase with the increase in H<sub>2</sub>O<sub>2</sub> concentration. The same experiments have been carried out with chloride-doped polypyrrole film-modified electrode and with bare electrode (data not shown). The minor effect of cathodic current increase was observed. Parent Dawson POMs have been found to not possess electrocatalytic activity to H<sub>2</sub>O<sub>2</sub> reduction.<sup>25</sup> Therefore Fe<sup>3+</sup>-substituted POM appears to be an exclusive electrocatalyst for H<sub>2</sub>O<sub>2</sub> reduction. Similar catalytic results were also obtained for the Cu<sup>2+</sup>-substituted POM-doped polypyrrole.

No increase of cathodic currents was observed at the Fe<sup>3+</sup>-substituted POM-doped film-modified electrode in the presence of dissolved oxygen. Thus the film reveals a sufficient selectivity towards peroxide electrochemical reduction.

The possible mechanism of the reduction of H<sub>2</sub>O<sub>2</sub> by Fe<sup>3+</sup>-POM-PPy film can be represented by the reactions in Scheme 1. In this inner sphere electron transfer reaction, the Fe<sup>III/II</sup> centre is actually responsible for the electron transfer pathway<sup>25</sup>. (Scheme 1)

##### Amperometry

The sensor performance of both the Fe<sup>3+</sup>- and Cu<sup>2+</sup>-POM doped polypyrrole films towards hydrogen peroxide was studied through amperometric experiments in stirred solution at -0.3V (vs Ag/AgCl) being chosen as the optimal applied potential. In contrast to the bare electrode and chloride-doped film-modified electrode, the increases in cathodic currents to 0.1 mM H<sub>2</sub>O<sub>2</sub> additions have been observed (Fig. 6) at both Fe<sup>3+</sup>- and Cu<sup>2+</sup>-POM doped film-modified electrodes.

The Fe<sup>3+</sup>-POM film-modified electrodes (surface coverages 10.8-11.3 nmol cm<sup>-2</sup>) showed a sensitivity of 0.5 A/(M\*cm<sup>2</sup>) with a limit of detection (LOD) of 0.56 μM based on a S/N ratio multiplied by 3. Steady state currents were obtained within 8 seconds from each injection. A linear range was observed between 0.1mM and 2 mM (r=0.999; n=20). Thinner films (surface coverages 3.0-4.2 nmol cm<sup>-2</sup>) revealed a sensitivity of 0.4 A/(M\*cm<sup>2</sup>), LOD 2.2 μM and linear ranges between 0.1 mM to 1 mM (r=0.999; n=10). Similar results were obtained with the Cu<sup>2+</sup>-POM film-modified electrodes. These POM-doped polypyrrole modified electrodes showed here exhibit LODs lower than the LODs of modified electrodes reported previously. Biosensor based on horseradish peroxidase entrapped within electrodeposited polypyrrole membrane showed the LOD 0.5μM with a linear range of 0.2mM<sup>59</sup>. Polypyrrole film doped with Keggin-type phosphomolybdate showed the LOD 0.5 μM with a sensitivity of 1.1 μA mM<sup>-1</sup><sup>60</sup>. Chemically synthesized polypyrrole modified with platinum nanoparticles revealed LOD 1.2 μM<sup>61</sup>. Silver nanoparticle-decorated polypyrrole colloids showed LOD 1.05 μM<sup>62</sup>.

#### Conclusions

Electrochemical polymerization of pyrrole and Fe<sup>3+</sup>-, Cu<sup>2+</sup>- and Co<sup>2+</sup>-substituted Dawson-type polyoxometalates as dopants has been carried out. Fe<sup>III/II</sup> redox process and Cu oxidation as well as three W-O redox processes associated with the incorporated POMs were observed against polymer backbone processes. The stabilization effect of the electrochemical response of the POMs due to immobilization into polypyrrole matrix has been observed. All electrode systems based on POMs immobilized into polypyrrole reveal sufficient pH dependencies. Different surface analysis techniques were used to characterize the surface morphologies of the obtained polymer membranes.

Electrocatalytic activity to hydrogen peroxide reduction observed at pH 6.5 for both Fe<sup>3+</sup>- and Cu<sup>2+</sup>-substituted Dawson POMs in polypyrrole matrix was employed for the development of an electrochemical peroxide sensor. Metal ion-substituted POM-doped polymer-modified electrodes reveal limits of detection lower than other previously reported modified electrode systems.

## Acknowledgement

The AFM, SEM and XPS analysis work was conducted under the framework of the INSPIRE programme, funded by the Irish Government's Programme for Research in Third Level Institutions, Cycle 4, National Development Plan 2007-2013

## Notes and references

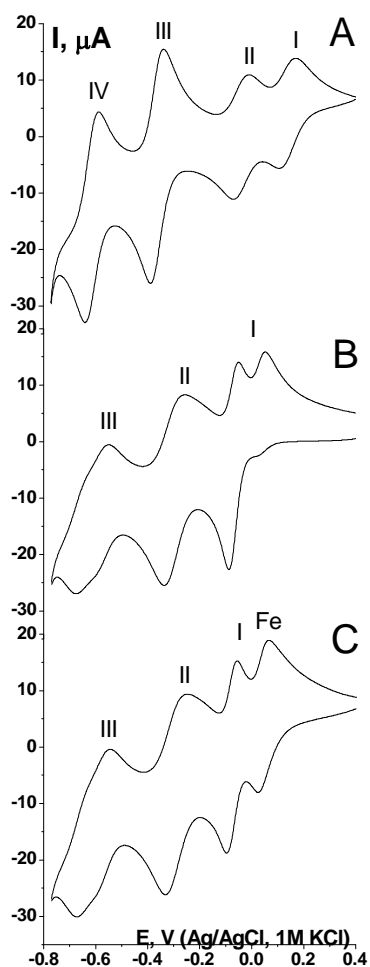
<sup>a</sup> *Electrochemistry Research Group, Department of Applied Science, Dundalk Institute of Technology, Dublin Road Dundalk, County Louth, Ireland. Fax: +353 42 933 1163; Tel: +353 42 937 4579; E-mail: tim.mccormac@dkit.ie*

<sup>b</sup> *Materials and Surface Science Institute, University of Limerick, Limerick, Ireland, Tel: +353 61 213127, Fax: + +353 61 213529*

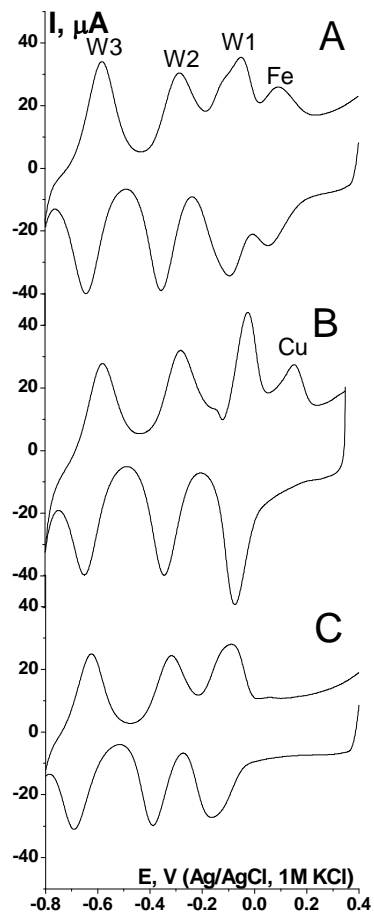
1. J. J. Borrás-Almenar, E. Coronado, A. Müller and M. T. Pope, *Polyoxometalate Molecular Science*, Kluwer Academic Publishers, Dordrecht, 2003.
2. N. Fay, E. Dempsey and T. McCormac, *Journal of Electroanalytical Chemistry*, 2005, **574**, 359-366.
3. C. L. Hill, *Comprehensive Coordination Chemistry II*, 2003, **4**, 679-759.
4. B. Keita, E. Abdeljalil, L. Nadjo, R. Contant and R. Belghiche, *Langmuir*, 2006, **22**, 10416-10425.
5. T. McCormac, B. Fabre and G. Bidan, *Journal of Electroanalytical Chemistry*, 1997, **427**, 155-159.
6. M. T. Pope, *Heteropoly and Isopoly Oxometalates*, Springer Verlag, New York, 1983
7. J. J. Borrás-Almenar, E. Coronado, A. Muller and M. T. Pope, *Polyoxometalates Molecular Science*, Kluwer, Dordrecht, 2004.
8. M. T. Pope and A. Muller, *Angewandte Chemie-International Edition in English*, 1991, **30**, 34-48.
9. M. T. Pope and A. Muller, *Polyoxometalates Chemistry: From Topology via Self Assembly to Application*, Kluwer Academic Publishers, Dordrecht 2001.

10. M. Sadakane and E. Steckhan, *Chemical Reviews*, 1998, **98**, 219-237.
11. T. Yamase and M. T. Pope, *Polyoxometalate Chemistry for Nano-Composite Design*, Kluwer Academic/Plenum Publishers, New York, 2002.
12. G. C. Yang, H. W. Guo, M. K. Wang, M. H. Huang, H. J. Chen, B. F. Liu and S. J. Dong, *Journal of Electroanalytical Chemistry*, 2007, **600**, 318-324.
13. P. Judeinstein, P. W. Oliveira, H. Krug and H. Schmidt, *Chemical Physics Letters*, 1994, **220**, 35-39.
14. C. Y. Rong and F. C. Anson, *Analytical Chemistry*, 1994, **66**, 3124.
15. C. Y. Rong and F. C. Anson, *Inorganica Chimica Acta*, 1996, **242**, 11-16.
16. B. Keita, L. Nadjo and R. Contant, *Journal of Electroanalytical Chemistry*, 1998, **443**, 168-174.
17. B. Keita, L. Nadjo, G. Krier and J. F. Muller, *Journal of Electroanalytical Chemistry*, 1987, **223**, 287-294.
18. M. A. Barteau, J. E. Lyons and I. K. Song, *Journal of Catalysis*, 2003, **216**, 236-245.
19. S. Y. Zhai, S. Y. Gong, J. U. Jiang, S. J. Dong and J. H. Li, *Analytica Chimica Acta*, 2003, **486**, 85-92.
20. G. Bidan, E. M. Genies and M. Lapkowski, *Synthetic Metals*, 1989, **31**, 327-334.
21. H. Y. Sung, H. S. So and W. K. Paik, *Electrochimica Acta*, 1994, **39**, 645-650.
22. D. E. Katsoulis, *Chemical Reviews*, 1998, **98**, 359-387.
23. M. J. Liu and S. J. Dong, *Electrochimica Acta*, 1995, **40**, 197-200.
24. T. McCormac, D. Farrell, D. Drennan and G. Bidan, *Electroanalysis*, 2001, **13**, 836-842.
25. S. J. Dong and M. J. Liu, *Journal of Electroanalytical Chemistry*, 1994, **372**, 95-100.
26. V. ThomeDuret, G. Reach, M. N. Gangnerau, F. Lemonnier, J. C. Klein, Y. N. Zhang, Y. B. Hu and G. S. Wilson, *Analytical Chemistry*, 1996, **68**, 3822-3826.
27. C. A. Marquette and L. J. Blum, *Analytica Chimica Acta*, 1999, **381**, 1-10.
28. O. Nozaki and H. Kawamoto, *Luminescence*, 2000, **15**, 137-142.
29. A. C. Pappas, C. D. Stalikas, Y. C. Fiamegos and M. I. Karayannis, *Analytica Chimica Acta*, 2002, **455**, 305-313.
30. J. Z. Li, P. K. Dasgupta and G. A. Tarver, *Analytical Chemistry*, 2003, **75**, 1203-1210.
31. S. A. G. Evans, J. M. Elliott, L. M. Andrews, P. N. Bartlett, P. J. Doyle and G. Denuault, *Analytical Chemistry*, 2002, **74**, 1322-1326.
32. A. A. Karyakin, E. A. Puganova, I. A. Budashov, I. N. Kurochkin, E. E. Karyakina, V. A. Levchenko, V. N. Matveyenko and S. D. Varfolomeyev, *Analytical Chemistry*, 2004, **76**, 474-478.
33. L. Q. Mao, P. G. Osborne, K. Yamamoto and T. Kato, *Analytical Chemistry*, 2002, **74**, 3684-3689.
34. A. A. Karyakin, E. E. Karyakina and L. Gorton, *Journal of Electroanalytical Chemistry*, 1998, **456**, 97-104.
35. F. Ricci and G. Palleschi, *Biosensors & Bioelectronics*, 2005, **21**, 389-407.
36. M. S. Lin and H. J. Len, *Electroanalysis*, 2005, **17**, 2068-2073.
37. A. Domenech and J. Alarcon, *Analytica Chimica Acta*, 2002, **452**, 11-22.

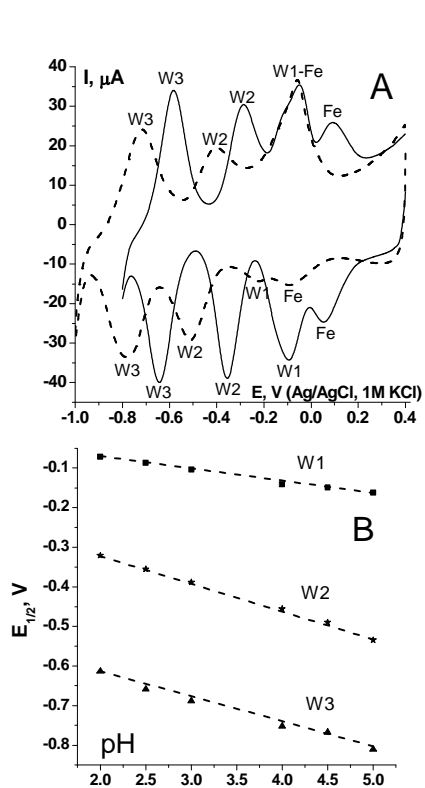
- 
38. P. Wang, X. P. Wang, L. H. Bi and G. Y. Zhu, *Journal of Electroanalytical Chemistry*, 2000, **495**, 51-56.
39. Y. C. Wu, R. Thangamuthu and S. M. Chen, *Electroanalysis*, 2009, **21**, 210-214.
- 5 40. A. K. M. Kafi, G. Wu and A. Chen, *Biosensors & Bioelectronics*, 2008, **24**, 566-571.
41. S. S. Razola, B. L. Ruiz, N. M. Diez, H. B. Mark and J. M. Kauffmann, *Biosensors & Bioelectronics*, 2002, **17**, 921-928.
42. V. G. Gavalas and N. A. Chaniotakis, *Analytica Chimica Acta*, 2000, **404**, 67-73.
- 10 43. L. H. Bi, K. Foster, T. McCormac and E. Dempsey, *Journal of Electroanalytical Chemistry*, 2007, **605**, 24-30.
44. A. Z. Ernst, S. Zoladek, K. Wiaderek, J. A. Cox, A. Kolary-Zurowska, K. Mieunikowski and P. J. Kulesza, *Electrochimica Acta*, 2008, **53**, 3924-3931.
- 15 45. J. E. Toth, J. D. Melton, D. Cabelli, B. H. J. Bielski and F. C. Anson, *Inorganic Chemistry*, 1990, **29**, 1952-1957.
46. H. Hamidi, E. Shams, B. Yadollahi and F. K. Esfahani, *Electrochimica Acta*, 2009, **54**, 3495-3500.
- 20 47. C. Q. Sun, J. H. Zhao, H. D. Xu, Y. P. Sun, X. Zhang and J. C. Shen, *Journal of Electroanalytical Chemistry*, 1997, **435**, 63-68.
48. K. Karnicka, M. Chojak, K. Miecznikowski, M. Skunik, B. Baranowska, A. Kolary, A. Piranska, B. Palys, L. Adamczyk and P. J. Kulesza, *Bioelectrochemistry*, 2005, **66**, 79-87.
- 25 49. M. Zhou, L. P. Guo, F. Y. Lin and H. X. Liu, *Analytica Chimica Acta*, 2007, **587**, 124-131.
50. I. M. Mbomekalle, R. Cao, K. I. Hardcastle, C. L. Hill, M. Ammam, B. Keita, L. Nadjo and T. M. Anderson, *Comptes Rendus Chimie*, 2005, **8**, 1077-1086.
- 30 51. D. K. Lyon, W. K. Miller, T. Novet, P. J. Domaille, E. Evitt, D. C. Johnson and R. G. Finke, *Journal of the American Chemical Society*, 1991, **113**, 7209-7221.
52. L. Ruhlmann and G. Genet, *Journal of Electroanalytical Chemistry*, 2004, **568**, 315-321.
- 35 53. C. L. Wang, S. X. Liu, C. Y. Sun, L. H. Xie, Y. H. Ren, D. D. Liang and H. Y. Cheng, *Journal of Molecular Structure*, 2007, **841**, 88-95.
54. P. Wang and Y. F. Li, *Journal of Electroanalytical Chemistry*, 1996, **408**, 77-81.
- 40 55. W. Y. Tao, Z. F. Li, D. W. Pan, L. H. Nie and S. Z. Yao, *Journal of Physical Chemistry B*, 2005, **109**, 2666-2672.
56. X. Y. Cui, J. F. Hetke, J. A. Wiler, D. J. Anderson and D. C. Martin, *Sensors and Actuators a-Physical*, 2001, **93**, 8-18.
57. T. Silk, Q. Hong, J. Tamm and R. G. Compton, *Synthetic Metals*, 1998, **93**, 59-64.
- 45 58. T. Silk, Q. Hong, J. Tamm and R. G. Compton, *Synthetic Metals*, 1998, **93**, 65-71.
59. F. Tian, B. Xu, L. Zhu and G. Zhu, *Analytica Chimica Acta*, 2001, **443**, 9-16.
- 50 60. X. Wang, H. Zhang, E. Wang, Z. Han and C. Hu, *Materials Letters*, 2004, **58**, 1661-1664.
61. X. Bian, X. Lu, E. Jin, L. Kong, W. Zhang and C. Wang, *Talanta*, 2010, **81**, 813-818.
62. X. Qin, W. Lu, Y. Luo, G. Chang and X. Sun, *Electrochemistry Communications*, 2011, **13**, 785-787.
- 55



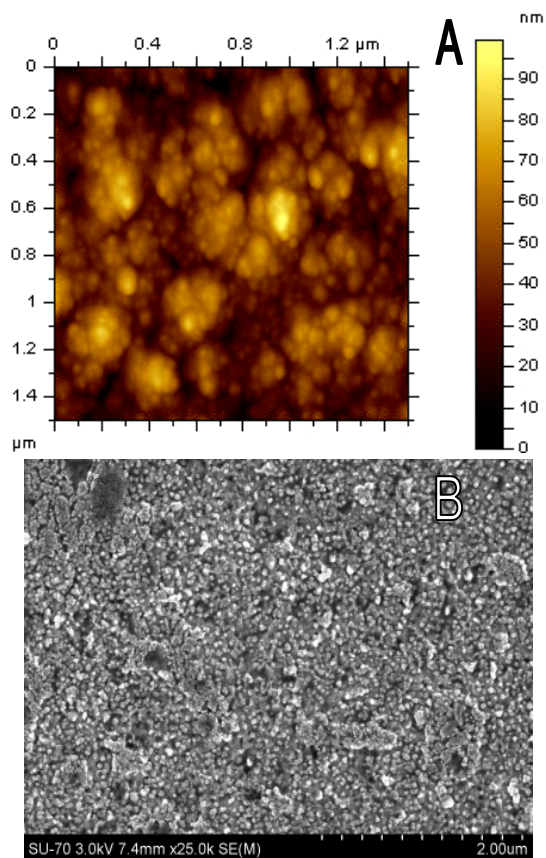
**Fig. 1** Cyclic voltammograms of POMs at different stages of  $\text{Fe}^{3+}$  ion insertion. A – parent Dawson, B – lacunary Dawson and C –  $\text{Fe}^{3+}$ -substituted Dawson. 1mM POM, 0.1M  $\text{Na}_2\text{SO}_4$ , pH2, 50 mV/s.



**Fig. 2** Cyclic voltammograms of POMs entrapped into polypyrrole film. A –  $\text{Fe}^{3+}$ -substituted, B –  $\text{Cu}^{2+}$ -substituted and C –  $\text{Co}^{2+}$ -substituted. 1mM POM, 0.1M  $\text{Na}_2\text{SO}_4$ , pH2, 50 mV/s.

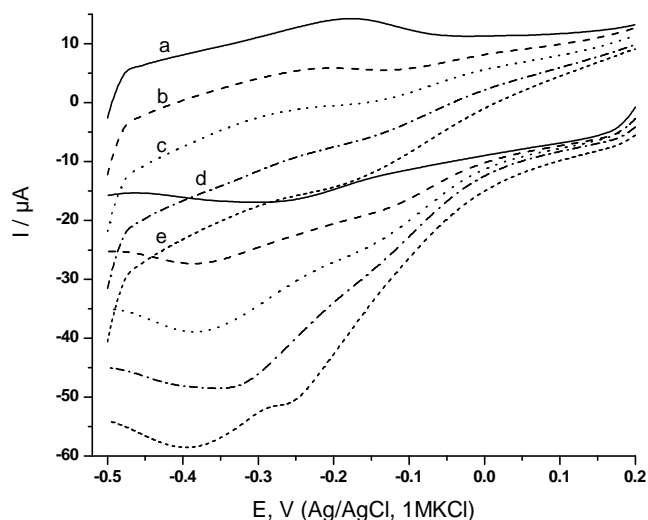


**Fig. 3** pH dependence of Fe<sup>3+</sup>-substituted POM entrapped into polypyrrole film. A – cyclic voltammograms obtained at pH 2.0 (solid line) and pH 4 (dashed line). 0.1M Na<sub>2</sub>SO<sub>4</sub>, 20mM CH<sub>3</sub>COOH, pH 2, 50 mV/s. B – the pH dependence of observed formal potentials.

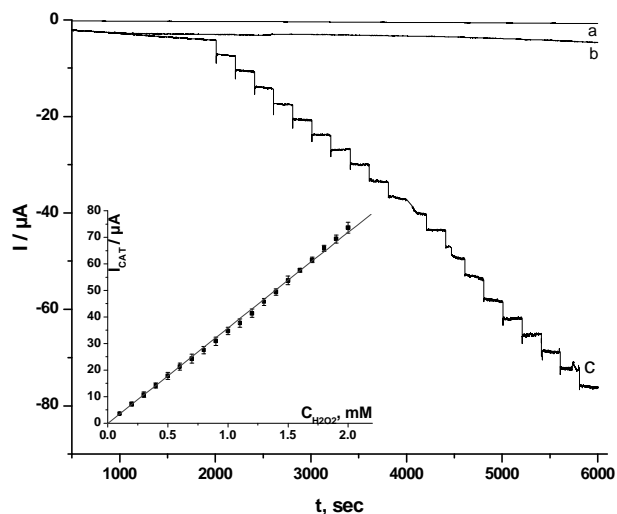


**Fig. 4.** AFM (A) and SEM (B) images of Co<sup>2+</sup>-doped polypyrrole film (10mC) on ITO coated glass slide;

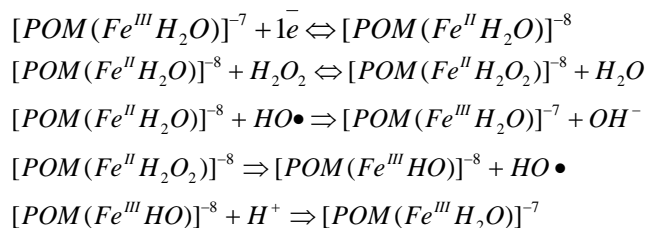




**Fig. 5** Electrocatalytic reduction of hydrogen peroxide at  $\text{Fe}^{3+}$ -substituted POM-doped polypyrrole film immobilized into electrode surface: a - 0 mM, b - 1 mM, c - 2 mM, d - 3 mM and e - 4 mM hydrogen peroxide. 0.1M  $\text{Na}_2\text{SO}_4$ , 20mM  $\text{NaH}_2\text{PO}_4$ , pH 6.5, 5mV/s.



**Fig. 6** Amperometric responses to hydrogen peroxide reduction. (a) – blank glassy carbon electrode, (b) – electrode modified with chloride-doped polypyrrole and (c) - electrode modified with  $\text{Fe}^{3+}$ -substituted POM-doped polypyrrole. Potential -0.3V, successive additions of 0.1 mM hydrogen peroxide, stirred 0.1M  $\text{Na}_2\text{SO}_4$ , 20mM  $\text{NaH}_2\text{PO}_4$  solution, pH 6.5. Inset: calibration plot of ( $n=3$ ).



**Scheme 1** Possible mechanism of  $\text{H}_2\text{O}_2$  reduction by  $\text{Fe}^{\text{III}}$ -POM, where POM –  $\text{P}_2\text{W}_{17}\text{O}_{61}$ .